**Canadian Journal of Civil Engineering**

# Analysis of Safety of Slender Concrete Masonry Walls in Relation to CSA S304-14

SCHOLARONE™
Manuscripts

1    Analysis of Safety of Slender Concrete Masonry Walls in Relation to CSA S304-14

2    Isfeld, Andrea C.[1], Müller, Anna Louisa[2], Hagel, Mark[3], and Shrive, Nigel G.[4]

3    1 Postdoctoral Scholar, Department of Civil Engineering, Schulich School of Engineering, 2500

4    University Drive NW, AB, Canada, acisfeld@ucalgary.ca

5    2  Research Associate, Department of Civil Engineering, Schulich School of Engineering, 2500

6    University Drive NW, Calgary, AB, Canada, anna_l_mueller@gmx.de

7    3 Executive Director, Alberta Masonry Council, P.O.Box 44023, RPO Garside, Edmonton, AB,

8    Canada, markhagel@albertamasonrycouncil.ca

9    4 Professor, Department of Civil Engineering, Schulich School of Engineering, 2500 University

10   Drive NW, Calgary, AB, Canada, ngshrive@ucalgary.ca

11   Corresponding Author: Andrea C. Isfeld, 2500 University Drive NW, AB, Canada,

12   acisfeld@ucalgary.ca, (403)220-2176

13   Word count: 7040

1    **ABSTRACT**

2    The Canadian masonry design standard appears to be overly conservative in determining the

3    capacity of concrete block walls with slenderness ratios greater than 30. When assessing the

4    potential for buckling of a masonry wall according to Euler buckling criteria, the effective height

5    is determined in part from the end supports. In Euler theory only pinned, fixed and free support

6    conditions are considered, and the Canadian standard considers the support conditions to be

7    hinged, elastic or stiff. For a partially reinforced masonry wall a true hinged base support is

8    expected to be difficult to achieve, as the width of the concrete block restrains rotation. The

9    effect of the base support conditions on the deflected shape of partially grouted block walls was

10   investigated under axial and out-of-plane loading. The results of this testing were compared with

11   calculations based on the Canadian masonry standard. It becomes clear that the standard is

12   overly conservative in many cases and the design of slender walls needs to be re-examined.

13

1 **INTRODUCTION**

2 Masonry is one of the oldest building materials. Ancient masonry structures were often over-

3 dimensioned due to the empirical design approach. In 1965 the National Building Code of

4 Canada was introduced, modeled on the British Code. The code contained rules for the design of

5 masonry by analysis of forces, moments, slenderness and stresses and produced the first

6 "engineered masonry" in Canada. As a result, masonry is slowly becoming competitive with

7 other building materials as design provisions are improved and expanded through experimental

8 research. However, when adhering to the current Canadian masonry design standard, CSA S304-

9 14 (2014), there are significant obstacles to the design of masonry walls subjected to axial and

10 out-of-plane loading with slenderness ratios greater than 30.

11 Material strength generally governs the resistance of reinforced and unreinforced concrete

12 masonry walls with low slenderness ratios, whereby axially loaded members fail by vertical

13 splitting, and the addition of a moment results in failure by crushing on the compression face

14 (Hatzinikolas et al. 1978). For this to be the case, the slenderness must be less than the limiting

15 value based on the end eccentricities, $e_1$ and $e_2$. The slenderness ratio is a function of the

16 effective length factor, k, wall height, h, and wall thickness, t. With increasing slenderness it is

17 necessary to account for secondary moment effects. When the slenderness ratio, kh/t, is below

18 30, CSA S304-14 (2014) permits a maximum resistance for pure axial load of 80% of the axial

19 capacity, based on material strength. However, when the slenderness ratio exceeds 30 according

20 to CSA S304-14 (2014) a wall design is permissible only if the applied factored axial load is

21 10% of the axial capacity or less. Thus, while it is known that the loadbearing capacity of a wall

22 decreases with increasing wall height, as failure can occur due to buckling (Chapman and

23 Slatford 1957; Drysdale and Hamid 2005), the standard enforces a drastic decrease in capacity at

3

1    a slenderness of 30 (from 80% to 10%). This approach is unique to masonry, and it has

2    previously been proposed that this reduction factor be a continuous function of the slenderness

3    (Ojinaga and Turkstra 1982) as is the case for the concrete design standard CSA A23.3-14

4    (2014). CSA S304-14 (2014) requires that all walls must be designed to resist a moment greater

5    than or equal to the axial load acting at a minimum eccentricity of 10% of wall thickness. In

6    addition to the primary moments causing out-of-plane displacements, additional bending

7    moment develops when the axial load at the supports acts over that displacement. The additional

8    moment causes the displacement to increase which in turn, leads to a further increase in the

9    moment.  The result is a second order load-displacement (P-$\Delta$) effect.

10   One factor affecting the permissible capacity of walls with a slenderness ratio greater than 30 is

11   the requirement for the assumption of pinned-pinned end conditions. The effective height factor

12   depends on the support conditions at the top and bottom of the wall and is used to determine the

13   effective height of the wall, kh. For a pinned-pinned (hinged-hinged as per CSA S304-14 (2014))

14   support condition, k is 1.0, whereas for a fixed-pinned (stiff-hinged) support condition, k is

15   reduced to 0.81. The smallest permissible value for k is 0.80 for walls that are fixed-fixed (stiff-

16   stiff).   Previous testing has focused on walls supported by a pinned connection at their base.

17   This approach is superior for understanding the material behaviour under well-established

18   conditions, however a pinned base support represents a theoretical condition found to deviate

19   from those used in practice (McDowell et al. 1956; Sahlin 1971; Hendry 1990; Yokel et al.

20   1971).  In this study, partially grouted, reinforced masonry walls were tested using realistic loads

21   for masonry tall walls supporting a lateral load and roof load, to help understand the degree to

22   which a reinforced concrete masonry wall can resist moment at its base when no additional effort

23   has been made to ensure a stiff, moment connection.

4

1    **PREVIOUS TESTING**

2    To assess the margin of safety provided by the provisions of CSA S304-14 (2014), previous

3    experimental studies of reinforced concrete masonry were reviewed, and experimental failure

4    loads compared to the capacities calculated using the Canadian standard. Experimental tests have

5    been completed on full-scale slender concrete block masonry walls subjected to axial loading by

6    Yokel et al. (1970), Cranston and Roberts (1976), Drysdale et al. (1976), Fattal and

7    Cattaneo (1976), Hatzinikolas et al. (1978), Suwalski (1986), Hatzinikolas et al.(1991), Mohsin

8    and Elwi (2003) and Liu and Hu (2007).  There have been a few experimental studies where the

9    walls were tested under a combination of out-of-plane and axial loading; including Yokel et

10   al. (1971), Fattal and Cattaneo (1976), the ACI-SEASC Task Committee on Slender Walls

11   (1982) and Popehn et al. (2008).  Tests have been primarily completed with pinned-pinned

12   boundary conditions.  Yokel et al. (1970) tested walls with the base supported fixed from

13   rotating (pinned-fixed), whereas Yokel et al. (1971) tested walls with a partially fixed base, and

14   Cranston and Roberts (1976) examined one wall that was fixed at both the bottom and the top.

15   The bottom support stiffness of the walls tested by Mohsin and Elwi (2003) varied between a

16   pinned support and a partially fixed support with a maximum stiffness of 10,000 kNm/rad.  Wall

17   heights have ranged from 2.5 to 7.4 m and slenderness ratios have varied from 12.9 to 51.2. In

18   cases where combined loading was used, axial load was applied before the walls were loaded to

19   failure with horizontal out-of-plane pressure.

20   While almost all studies involved testing walls with pinned support conditions at both the bottom

21   and the top of the wall, in reality, masonry walls do not have free rotation at the base. Addressing

22   the problem of unrealistic boundary conditions, in-situ testing has been completed by Dizhur et

23   al. (2009) to assess the strength and stiffness of brick masonry under quasi static out-of-plane

5

1    loading, and by Walsh et al. (2017) to assess the seismic out-of-plane behaviour of unreinforced

2    brick masonry with varied geometric configurations and boundary conditions. Dizhur et al.

3    (2009) found the flexural stiffness of in-situ walls to be much larger than that obtained from

4    laboratory built specimen, while Walsh et al. (2017) showed that fixing the top support resulted

5    in increased out-of-plane capacity due to arching action, while two-way flexure further increased

6    the load carrying capacity.  This is consistent with what was previously observed by McDowell

7    et al. (1956) whereby fixed end tests had 3-6 times the load carrying capacity of pinned end tests.

8    Arching action has been observed to increase the out-of-plane strength of walls bounded by rigid

9    elements such as reinforced concrete frames, while this behaviour is less likely with more

10    flexible wood diaphragms.  The base support of masonry walls is a hybrid of fixed and pinned

11    conditions rather than behaving as a distinct pin.

12    ***Previous testing walls summary***

13    Walls tested under axial load alone are outlined in Table 1. The height of these walls varied

14    between 2.4 and 6.4 m with slenderness ratios from 17.1 to 42.7. The axial load was increased

15    until failure occurred. The eccentricity of the load at the top of the wall is indicated by $e_1$, while

16    $e_2$ denotes the eccentricity at the bottom. Test conditions that allowed rotation at the bottom as

17    well as at the top of the wall are listed as pinned-pinned support conditions and a pinned-fixed

18    condition means that the rotation at the bottom of the wall was restricted. Typical end

19    eccentricities ranged from 1/6 to 1/3 of the thickness of the unit. For reinforced masonry walls

20    eccentricities up to 0.5t were used, and in the study of Suwalski (1986) even up to 0.75t. Most

21    commonly, the walls were subjected to equal end eccentricities ($e_1/e_2 = 1$). For equal bottom and

22    top support conditions, this load arrangement forced the wall to bend in symmetrical single

23    curvature and caused the maximum stress at the mid-height of the wall. For $e_1/e_2 = 0$ the

6

1    eccentricity at the bottom was zero and for $e_1/e_2 = -1$ end eccentricities were aligned in different

2    directions. These test conditions caused the walls to bend in asymmetrical single curvature and in

3    double curvature, respectively.

4    Unlike the testing of walls subjected only to axial loads, few experimental studies have been

5    completed where the walls were tested under a combination of out-of-plane and axial loading.

6    Yokel et al. (1971), Fattal and Cattaneo (1976), the ACI-SEASC Task Committe on Slender

7    Walls (1982), Popehn et al. (2008) report on such testing. The characteristics of the walls,

8    loading and support conditions are summarized in Table 2. Wall heights ranged from 2.5 to 7.4

9    m with slenderness ratios from 12.9 to 51.2. Axial load was applied before the walls were loaded

10    to failure with out-of-plane pressure. In two studies the axial load was only applied

11    concentrically, and in the other two also eccentrically. Most tests focused on walls with pinned

12    supports top and bottom.

13    To determine if the Canadian standard is overly conservative, the experimental failure loads were

14    compared to the theoretical axial load and moment capacity according to CSA S304-14 (2014).

15    It must be noted that most of the walls tested appeared not to fail by buckling, but in various

16    forms of material compression failure. Inadequate spreading of the concentrated load into the

17    masonry appeared to be the cause of this failure in some test series, with the result that buckling

18    was rarely achieved. Thus the load to cause compressive or flexural failure corresponding to the

19    analysis method would have been higher than that recorded and consequentially the level of

20    conservatism of the standard as determined below is underestimated.

21    ***Results of walls subjected to axial loads***

22    For the walls subjected to axial load alone three values representing the axial load capacity were

23    calculated; the axial resistance, $P_r$, and critical axial load, $P_{cr}$, both based on CSA S304-14

7

1    (2014), and the theoretical Euler buckling load. The Euler load was calculated for comparison to

2    the critical axial load.  The critical axial load is used only for application of the moment

3    magnifier equation and is not intended to evaluate the potential for buckling. For calculation of

4    the Euler load the modulus of elasticity, E, and the initial second moment of area, $I_o$, were

5    needed. $I_o$ was determined from the section properties and E was either taken from the

6    experimental studies or, if no information was available, assumed to be $850f'_m$ as per CSA S304-

7    14 (2014). For the critical axial load, $P_{cr}$, the modulus of elasticity E was always set to $850f'_m$.

8    The wall details, the results of our calculations, and the experimental failure loads for different

9    loading conditions of the unreinforced walls tested by Hatzinikolas et al. (1978) are shown in

10   Table 3. Similar tables were created for all other authors whose results we analysed. The last

11   column of the table shows the ratio of the experimental failure load to the axial load resistance

12   according to the CSA S304-14 (2014).

13   Evaluation of the data shows that the buckling load calculated using Euler theory is far in excess

14   of both the experimental failure loads and the calculated critical axial load $P_{cr}$. This is expected

15   as the Euler buckling load is based on the behaviour of linear elastic materials and utilizes the

16   gross cross-sectional properties, while calculation of the critical axial load requires application of

17   reduction factors and a reduced flexural rigidity to represent the brittle failure of masonry in

18   tension; the resulting critical load is approximately 0.17 and 0.13 of the Euler load for

19   unreinforced and reinforced masonry walls respectively. For tall walls and walls with small

20   eccentricities, the critical axial load $P_{cr}$ calculated according to CSA S304-14 (2014) is much

21   smaller than the experimental failure load. For large eccentricities and thus smaller experimental

22   failure loads, the values of $P_{cr}$ can exceed the experimental failure loads.

1    Reinforced masonry walls with virtual eccentricities e ≤ t/3, whose cross-sections were mainly

2    under compression, were treated like unreinforced masonry walls. Comparison of the test results

3    and the predicted capacities showed that the ratios of the experimental to predicted failure loads

4    were generally between 2 and 4. Mohsin and Elwi (2003) tested walls with different support

5    stiffness at the bottom. As CSA S304-14 (2014) does not provide direction on calculating the

6    load-bearing capacity as a function of a rotational spring, the two borderline cases of pinned and

7    fixed conditions were considered. Even for an assumption of a fixed condition the standard is

8    conservative in the range of approximately 2.5 to 5.5. For very tall reinforced walls with small

9    eccentricities, such as those tested by Yokel et al. (1971) and Hatzinikolas et al. (1978), ratios

10   even reached values between 5 and 7. The results of Yokel et al. (1971) and Hatzinikolas et al.

11   (1978) indicate that there is a general trend for CSA S304-14 (2014) to be more conservative

12   with increasing wall height. Figures 1 and 2 show the ratios of experimental to calculated failure

13   load for walls of varying height for reinforced and unreinforced walls respectively.  The data are

14   divided by pinned-pinned (a) and pinned-fixed (b) boundary conditions and shown individually

15   for each test program with an overall trend indicated. The results show low statistical

16   significance, and the relationship between height and the ratio of experimental to calculated

17   failure load varies. The results are generally less conservative with increasing eccentricity: the

18   exception is the test results of Liu and Hu (2007), which showed increasing conservatism for

19   increasing eccentricities. Based on the test results of Hatzinikolas et al. (1978) the level of

20   conservatism appears to increase as the loading changes from single to double curvature. The

21   difference was particularly noticeable for large eccentricities. However, the test results of Fattal

22   and Cattaneo (1976) and Liu and Hu (2007) indicate the opposite trend.

1    *Results for walls subjected to combined out-of-plane and axial loads*

2    Experimental results of walls subjected to combined axial and out-of-plane loads were compared

3    to calculated load-moment interaction curves. In addition to the resistance curve, the acting

4    moments were plotted as a function of the axial load $P_r$. In contrast to the moments acting on

5    walls that were subject to axial load only, these moments were calculated by adding the moment

6    caused by the out-of-plane pressure and the axial load multiplied by the measured deflection of

7    the wall. Second order effects were thus taken into account. In the case of pinned-partially fixed

8    boundary conditions of Yokel et al. (1971), the partial fixity was accounted for by applying a

9    factor of 0.68 to the magnified pinned-pinned moment, as outlined by the authors. As an

10   example, the details and results of the walls tested by the ACI-SEASC Committee (1982) are

11   shown in Table 4. P indicates the applied vertical load, $M_r$ the moment resistance and $M_{f,tot}$ the

12   magnified acting moment according to CSA S304-14 (2014).  For the purpose of analysis a

13   margin of safety is defined as the ratio of the acting moment on the wall to the calculated

14   moment resistance $M_r$ based on CSA S304-14 (2014). Two examples of load-moment-interaction

15   curves are provided in Figure 3. Such curves were created for each wall tested by the different

16   authors.

17   The comparison shows that almost all of the experimental results fall outside the range that is

18   surrounded by the resistance curve. Yokel (1971) also tested several walls with axial loads that

19   went far beyond the theoretical axial load capacity. The ACI-SEASC Task Committe on Slender

20   Walls (1982) only applied small axial loads that were below the balance point. The

21   reinforcement was thus in the tension zone and reached its yield strength. Evaluation of all the

22   data shows that the standard underestimates capacity by values between 1 and 2 for small axial

23   loads, but by factors up to 13 for larger loads. The calculation cannot be performed for cases

10

1    where the applied axial load exceeded the predicted capacity, as hypothetically, the factor tends

2    to infinity. The same applies for unreinforced walls with no axial load and thus no moment

3    capacity. Yokel et al. (1971) also tested one of each wall type under axial load only, which

4    showed that the theoretical axial load capacity is between 2/5 and 3/5 of the experimental axial

5    load capacity. In addition to the actual acting moment, the magnified moment according to CSA

6    S304-14 (2014) was calculated to assess the moment magnifier method relating to walls under

7    combined out-of-plane and axial loads. The moments are in good agreement for small

8    slenderness ratios and small axial loads. However, for larger slenderness ratios and axial loads

9    the moment magnifier method considerably overestimates the acting moment.

10   ***Previous testing conclusions***

11   The review and analysis of experimental failure loads of concrete masonry walls confirmed that

12   the load-bearing capacity predicted by the CSA S304-14 (2014) provisions is conservative. For

13   reinforced walls subjected to axial loads only, the calculated capacity becomes more

14   conservative with increasing wall heights and decreasing load eccentricity, while the relationship

15   is less clear for unreinforced masonry walls. One reason for the underestimation of capacity is

16   the magnification of the acting moment. The magnification depends on the applied axial load and

17   the critical axial load, $P_{cr}$, which is a function of the effective flexural rigidity and the effective

18   height of the wall. Neglecting the rotational stiffness at the bottom of the wall will increase the

19   moment magnification compared to if it were accounted for. For masonry walls exposed to a

20   combination of out-of-plane and axial loading, the standard is especially conservative for load

21   cases involving large vertical loads. Comparison between the applied moments and the

22   theoretical moments determined with the moment magnifier method showed that the moment

23   magnifier method overestimates the acting moment for large axial loads and large wall heights.

11

1    While this analysis of previous studies has shown the CSA S304-14 (2014) calculations to give

2    conservative results for the theoretical boundary condition presented in the literature, this

3    problem is compounded by the fact that pinned base boundary conditions are not constructed in

4    practice. In order to improve the efficiency of the current design approach further testing is

5    needed to better understand the behaviour of slender masonry walls subjected to axial and out-of-

6    plane loading. To understand the ability of a slender reinforced concrete block masonry wall to

7    restrain moment at its base when a stiff moment connection is not imposed, testing of walls with

8    such a support is necessary. Comparison with pinned base behaviour is used to demonstrate how

9    the walls deviate from this theoretical condition in practice. By measuring the deflections along

10    the wall height, the displaced profile and maximum displacement were determined and compared

11    between walls, and with values calculated using the Canadian standard.

12    **TEST DESIGN**

13    Three concrete masonry walls were tested under axial and out-of-plane loading with both

14    pinned-pinned and what will be referred to as pinned-fixed boundary conditions. Testing was

15    first completed for a wall having pinned-fixed boundary conditions then the test set-up was

16    altered to test the same wall as pinned-pinned. This order was utilized to prevent damage to the

17    walls from occurring under the initial boundary conditions as larger displacements were

18    permitted with the pinned base support. Comparison of the out-of-plane displaced profiles was

19    used to evaluate the wall behaviour and compare the results with calculations based on CSA

20    S304-14 (2014) for both pinned-pinned and pinned-fixed end conditions.

21    *Wall specimens*

22    Three concrete masonry walls were built 2.4 m high by 1.2 m wide, with 15 MPa standard, bond

23    beam, and half block hollow concrete masonry units with an actual thickness of 190 mm (cross-

12

1  section shown in Figure 4).  The walls thus had a height to thickness ratio of 12.6, and

2  slenderness ratios of 12.6 and 10.2 for the pinned-pinned and pinned-fixed boundary conditions

3  respectively. The masonry was face-shell bedded and laid in running bond. The second cell from

4  each end of each wall was grouted and vertically reinforced with a 15 M (16 mm diameter)

5  reinforcing bar. In addition, the first, fifth and last (twelfth) courses were grouted and

6  horizontally reinforced with a 15 M reinforcing bar. The walls were constructed eccentrically in

7  steel C-channels with 600 mm 15 M starter bars welded to the base.  The vertical reinforcement

8  was lapped and tied to the starter bars.  The steel channel had 4 bolt tabs on each side to secure

9  the walls to the load floor, as shown in Figures 5 and 6.

10  *Materials*

11  The concrete block masonry units used were manufactured by Expocrete, being of actual size of

12  390 mm × 190 mm × 190 mm and nominal 15 MPa strength. The walls were constructed with

13  Type S mortar mixed by combining Portland cement, lime, sand and water according to CSA-

14  A179-2014, using the pre-bagged Spec Mix product described in Table 5.  The grout was mixed

15  according to proportion specification of CSA-A179-2014 using the pre-bagged Blockfill product

16  described in Table 6.

17  *Compression testing*

18  Individual grout cylinders, mortar cubes, and masonry prisms were constructed for compressive

19  testing at 28 days post construction and on each testing date.  Individual concrete block units

20  were also tested for compressive strength.  Masonry prisms were hollow, 2 units high, and cured

21  under the same conditions as the full walls.  The mortar cubes were cured beneath polyethylene

22  sheets.  Grout cylinders were cured at 100% humidity and 23°C until testing. Prisms were

23  capped on the face shells with Plaster of Paris as outlined in Annex D (D.4.1) of CSA S304-14

1    (2014).  The top and bottom surfaces of the grout cylinders were ground to achieve a flat surface

2    for testing.  The material properties obtained are summarized in Table 7 with the coefficient of

3    variation (C.O.V.) and corrected compressive strengths based on an effective C.O.V. of 10%

4    when less than 10 samples were tested, as outlined in Annex C of CSA S304-14 (2014).

5    *Test arrangement*

6    The test arrangement was a modified version of the vertical test for transverse loading in ASTM

7    E72 (2015). The three walls were each tested with both the pinned-fixed and pinned-pinned

8    boundary conditions. The walls were subjected to a combination of eccentric axial load and an

9    out-of-plane line load, which was applied to specific magnitudes in order to evaluate the

10   displaced profile.  Axial load was applied through two actuators in displacement control up to a

11   maximum load of 250 kN (208 kN/m).  This load was distributed over the wall width through an

12   I-beam between the actuators and the 50.8 mm diameter round bar (Figure 5).  As indicated in

13   Figure 5 and 6(a), out-of-plane bracing was used to restrain sway of the loading beam.  Threaded

14   rods and cables within the bracing system were adjusted to eliminate any out-of-plane

15   displacements that occurred at the top roller during loading. To avoid local material failure, it

16   was necessary to spread the line load from the rod to the whole cross-section of the wall at both

17   the top and base of the wall. To facilitate this load spreading, two sets of four steel plates were

18   welded together to have a total thickness of 100 mm each and were placed on top of the last

19   course and below the C-channel on which the walls were built.  The C-channel was positioned

20   concentrically below the loading frame, thus placing the wall at an eccentricity of t/3. Pinned

21   base and top supports were provided using steel bars upon which the steel plates could rotate:

22   steel blocking was used to fill the gap between the steel plates at the base support as seen in

23   Figure 5 and 6(b) to create the fixed support condition when that was desired.  During the

14

1    pinned-fixed testing rotations of the C-channel were further restrained by threaded rods which

2    connected tabs on the C-channel to the lab floor; nuts were tightened above and below the tabs.

3    To prevent the threaded rods from restraining rotation during pinned-pinned testing the

4    connecting tabs had slotted holes and the nuts were loosened.  The details for each base support

5    conditions are shown in Figure 5.

6    An out-of-pane line load was applied at mid height by means of a box beam that was pulled

7    against the wall. Steel cables were fixed to both ends of the box beam and were connected with a

8    turnbuckle. The direction of the cables was changed with pulleys that were attached to steel

9    columns. Tightening the turnbuckle led to tension in the steel cables, which pulled the box beam

10   against the wall. The force in the steel cable was measured via a load cell, implemented by

11   gluing strain gauges to the turnbuckle.  The tension in the cable was increased to 6.3 kN, thus

12   applying a 12.6 kN out-of-plane force to the wall. Two walls were taken to the full 250 kN axial

13   load and 12.6 kN out-of-plane load and the third wall was taken to 50% (P = 125 kN and $w_{oop}$ =

14   5.29 kN/m), 75% (P = 187.5 kN and $w_{oop}$ = 7.94 kN/m), and 100% (P = 250 kN and $w_{oop}$ = 10.58

15   kN/m) of these loads to collect data on the out-of-plane displacements.  The cases of axial load

16   alone and combined axial and out-of-plane loads were applied for both the pinned-pinned and

17   pinned-fixed support conditions for all three walls - twelve tests in all.

18   To collect data for the displaced profile out-of-plane displacements were measured at four points

19   along the wall height (equally spaced at 480 mm increments) using laser displacement sensors

20   with a resolution of 1 μm, and at the level of the top support using a LVDT. Rotation of the top

21   of the wall with respect to the loading beam was recorded using the relative displacements on

22   either side of the roller using LVDTs.  Preliminary testing indicated the sensitivity of the setup to

23   small out-of-plane displacements at the top of the wall due to the flexibility of the bracing.  To

1    correct for this displacement the threaded rod was extended or the cable was tensioned until the

2    top support was returned to zero displacement.  During this iterative process the out-of-plane and

3    vertical loads were adjusted to maintain the test loads.

4    *Results*

5    The flexibility of the frame was such that even with the out-of-plane bracing system it was not

6    possible to reduce the lateral displacement of the top support completely to zero as shown for

7    one data set in Figure 7.  For consistency when comparing the results it was necessary to zero all

8    data using a linear offset.  The offset was determined by the slope of the line, m, connecting the

9    two supports.

10   $$m = \frac{D_{top}}{H_{total}} \tag{1}$$

11   Where $D_{top}$ is the displacement at the top roller and $H_{total}$ is the height of the wall from base

12   support to the centroid of the top roller.

13   The data from each of the three walls were used to plot an envelope of the maximum and

14   minimum displacements under each load combination and boundary condition for all walls. The

15   displacements are plotted in Figures 8 through 11 for the fixed and pinned base supports when

16   subjected to axial and out of plane load as indicated.  For the pinned-pinned condition, the

17   maximum displacement consistently occurred at the mid-height of the wall as shown in Figure 8

18   and 9.  In contrast, when the walls were tested in the pinned-fixed condition, the maximum

19   displacement was consistently above the mid-height as shown in Figure 10 and 11.  When

20   eccentric axial load was applied to the pinned-fixed wall alone, the location of the maximum out-

21   of-plane displacement occurred near 0.8H (80% of the total height).  The addition of the out-of-

22   plane line load at H/2 caused a significant increase in the out-of-plane displacement and the

23   maximum displacement appeared to shift to a lower position in the walls, as may be seen by

16

1    comparing Figure 10 and 11. It was not possible to specify the precise location of the maximum

2    displacement as displacements were only measured at specific heights.

3    Cracking was observed during the pinned-pinned testing under the combined axial and out-of-

4    plane loading.  The displacement profiles of Wall 3 were therefore determined at 50%, 75%, and

5    100% of the test loads to assess the effect of cracking.  No cracking was observed during the

6    pinned-fixed tests which were completed first.  Cracking was initiated in the pinned-pinned test

7    at 75% of the maximum axial and out-of-plane load with opening at the exterior edges of the

8    horizontal mortar joint at the mid-height of the wall.  Additional mortar joints above and below

9    mid-height were observed to open when the vertical load was applied alone at 100%, followed

10   by significant joint opening at the full vertical and out-of-plane loading.

11   The results of the pinned-pinned testing at 50% and 75% of the axial and combined loads are

12   shown in Figures 8 and 9 respectively.  The displacements increase from 0.8 mm to 1.4 mm

13   when the axial load is increased from 50% to 75%.  The displacements under 100% of the axial

14   load were in the range of 1.9 to 3.8 mm.  At 50% of the combined out-of-plane and vertical load

15   the mid-height of the wall displaces 2.5 mm. This displacement increases to 4.4 mm under 75%

16   of the combined total load and to 6.6 mm to 9.8 mm under 100% of the combined load, showing

17   the sensitivity of pinned-pinned walls to out-of-plane loads, and the effect of the cracking.

18   The results of the pinned-fixed testing at 50% and 75% of the axial and combined loads are

19   shown in Figure 10 and 11.  The fixed base support reduces the sensitivity of the wall to out-of-

20   plane loading.  At 50% of the total axial load the maximum displacement was 0.3 mm which

21   increased to 0.6 mm at 75%. In Figure 11 it is shown that the maximum displacement increases

22   from 0.5 mm to 1.1 mm when the loads are increased from 50% to 75% of the combined total.

23   From Figure 10 it can be seen that the maximum displacement under 75% of the axial load falls

17

1   within the 100% axial envelope. The same is true when axial and out-of-plane loads are applied,

2   as shown in Figure 11. The small displacements under these pinned-fixed conditions are highly

3   sensitive to errors in the measurement system and a discrepancy in the results can be seen at

4   0.4H under 50% of the total combined loads. This error could be introduced due to contact with

5   the laser supports during the process of adjusting the top out-of-plane displacements.

6   The ratio of the displacements for the pinned-pinned and pinned-fixed loading conditions were

7   calculated from the maximum displacement for each bounding profile and are provided in Table

8   8. The ratio is found to increase with the applied loads. This is due to the increased P-Δ effect

9   under higher loads when the base of the wall is pinned, the occurrence of crack opening at large

10   loads, and experimental error being more significant when the displacements are small. The

11   effect of experimental error is greatest for the pinned-fixed wall under 50% of axial load alone.

12   Having used only 4 points of measurement in the test set-up prevents the absolute maximum

13   values from being collected, particularly for the pinned-pinned case where the maximum

14   displacement would occur at mid-height. Overall, the ratio of pinned to fixed displacements is in

15   the range of 1-5 prior to cracking of the pinned model. After cracking was observed the ratio

16   increased to 8.3.

17   **CALCULATION OF DISPLACEMENT**

18   In CSA S304-14 (2014) displacements are calculated using the service loads. Calculation of the

19   service displacements are required for walls subjected to lateral wind loads when the wall span

20   exceeds 25d. The standard provides a simplified method for calculating the mid-height

21   deflection. For walls with a slenderness ratio less than 30, the option is also given for rational

22   analysis based on engineering practice and theory. Secondary moment effects can be

23   approximated using the moment magnifier method. Alternatively, the moment is magnified using

18

1    the P-Δ method whereby the displacement under the applied moment is calculated and updated

2    with the additional moment attributed to the axial load acting at an increasing eccentricity due to

3    the out-of-plane displacements.  Using the P-Δ method the final moment and displacement are

4    found once the solution has converged.

5    *Displacement calculations*

6    When the service moment at mid-height of the walls, $M_s$, is less than the cracking moment the

7    displacement is calculated using the simplified approach as

8
$$\Delta = \frac{5 M_s H_w^2}{48(EI)_o} \tag{2}$$

9    Where $H_w$ is the height of the wall and $(EI)_o$ is the gross cross-sectional stiffness. For this test

10   assembly the wall height is taken between pinned supports as 2.67 m and from the pinned to

11   fixed support as 2.54 m.  When the service moment is greater than the cracking moment the

12   displacement is calculated as

13
$$\Delta = \frac{5 M_{cr} H_w^2}{48(EI)_o} + \frac{5(M_s - M_{cr})H_w^2}{48(EI)_{cr}} \tag{3}$$

14   Where $(EI)_{cr}$ is the cracked stiffness and $M_{cr}$ is the cracking moment.

15   As an alternative to the simplified approach for displacement calculation, more detailed analysis

16   is permitted.  These calculations will be outlined for both the pinned-pinned and pinned-fixed

17   support conditions. For the wall with pinned-pinned conditions the maximum displacement was

18   calculated at mid-span using the following equation for equal end moments, caused by the

19   service load, $P_s$, acting at an eccentricity, $e_p$, and out-of-plane line load, $w_{oop}$, acting on the

20   effective width, $b_{eff}$.

21
$$\Delta_{p-p} = \frac{w_{OOP} b_{eff} H_w^3}{48(EI)_{eff}} + \frac{e_p P_s H_w^2}{8(EI)_{eff}} \tag{4}$$

1    Where $(EI)_{eff}$ is the effective stiffness.

2    For a pinned-fixed wall the location of maximum displacement is calculated by finding the roots

3    of the first derivative of the equation for the displacement at any location on the wall. The

4    equation for the displacements at the location x from the top of the wall is

5
$$\Delta_{p-f} = \frac{e_p P_s}{4(EI)_{eff}H_w}\left(-x^3 + 2x^2 H_w - xH_w{}^2\right) + \frac{w_{OOP}b_{eff}}{96(EI)_{eff}}\left(5x^3 - 3xH_w{}^2\right) \qquad (5)$$

6    The distances from the top of the wall for maximum displacement were 845 mm and 948 mm for

7    the axial case and the combined axial and out-of-plane load case respectively (ie: at heights of

8    1.7 m (0.67H) for axial alone and 1.6 m (0.626H) for axial plus lateral load).

9    ***Section properties***

10   The sections properties $(EI)_o$ and $(EI)_{cr}$ are used to determine the effective property $(EI)_{eff}$. The

11   second moment of area for the gross cross section, $I_o$, is based on the partially grouted,

12   reinforced section. The cracked section modulus is calculated based on the cross sectional

13   properties as

14
$$I_{cr} = \frac{1}{3}b_{eff}(kd)^3 + nA_{s,eff}(d - kd)^2 \qquad (6)$$

15   Where $A_{s,eff}$ is the area of steel within the effective length of the wall $b_{eff}$. The steel is located at

16   a distance d from the compression face, which is t/2 for a symmetric section. The cracked

17   second moment of area, $I_{cr}$, is calculated either including or excluding the grout based on

18   whether the length kd is found to be within the face shell thickness using the moment area

19   method as

20
$$kd = \left(\sqrt{(n\rho)^2 + 2n\rho} - n\rho\right)d \qquad (7)$$

21   Where $\rho$ is the reinforcement ratio

20

1
$$\rho = \frac{A_S}{bd} \qquad (8)$$

2  The ratio of moduli, n, is

3
$$n = \frac{E_S}{E_m} \qquad (9)$$

4  The modulus of the masonry, $E_m$, is related to the effective compressive strength according to the

5  equation in CSA S304-14 (2014).  For a partially grouted wall the effective compressive strength

6  is calculated based on weighted averages of hollow and solid $f'_m$ values given in Table 4 of CSA

7  S304-14 (2014). The same expression can be applied when determining the modulus of the

8  hollow masonry using $f'_{m,hollow}$ if the length kd is found to be less than the thickness of the

9  flange, $t_f$.

10
$$E_m = 850 f'_{m,eff} \qquad (10)$$

11

12  The first method for calculating the effective stiffness is adapted from that used for strength

13  calculations, which is related to the kern eccentricity for the section, $e_k$, and the load eccentricity,

14  e.

15
$$(EI)_{eff,1} = 0.25(EI)_o - (0.25(EI)_o - (EI)_{cr})\left(\frac{e - e_k}{2e_k}\right) \begin{array}{c} \leq 0.25(EI)_o \\ \geq (EI)_{cr} \end{array} \qquad (11)$$

16  Where the load eccentricity is calculated based on the service moment and load rather than the

17  factored loads as

18
$$e = \frac{M_S}{P_S} \qquad (12)$$

19  And the kern eccentricity is calculated from the geometric properties as

20
$$e_k = \frac{S_e}{A_e} = \frac{I_o}{y_t A_e} \qquad (13)$$

1 Where $S_e$ is the section modulus, $A_e$ is the gross area, $I_o$ is the gross second moment of area, and

2 $y_t$ is the distance from the neutral axis to the extreme tension fibre of the uncracked section

3 which is equal to t/2 for a symmetric section.

4 Using the first approach the effective stiffness $(EI)_{eff,1}$ is limited to a maximum of $0.25(EI)_o$ and

5 can lead to falsely high displacements. As an alternative, for serviceability conditions the

6 effective stiffness, $(EI)_{eff,2}$, may be found based on the cracking moment, the service moment,

7 and the cracked and gross section modulus as

8
$$(EI)_{eff,2} = \frac{M_s}{\frac{M_{cr}}{(EI)_o} + \frac{M_s - M_{cr}}{(EI)_{cr}}} \tag{14}$$

9 The cracking moment is calculated as

10
$$M_{cr} = \frac{(f_t + f_{cs})I_o}{y_t} \tag{15}$$

11 where $f_{cs}$ is the axial compressive stress due to un-factored axial loads and $f_t$ is the flexural

12 tensile strength based on the weighted average of the values from Table 5 of CSA S304-14

13 (2014) for grouted and hollow concrete block with tension normal to the bed joints.

14 When the moment magnifier method is used to account for secondary moment effects the

15 magnified moment, $M_{s,mag}$, replaces the service moment, $M_s$, in equations (2) through (5). The

16 moment magnifier equation is applied as follows.

17
$$M_{s,mag} = M_s \frac{C_m}{\left(1 - \frac{P_s}{P_{cr}}\right)} \tag{16}$$

18 where $C_m$ is factor relating the actual moment diagram to an equivalent moment diagram, using

19 the end moments $M_1$ and $M_2$ where $M_1 \leq M_2$.

22

1
$$C_m = 0.6 + 0.4\frac{M_1}{M_2} \geq 0.4 \qquad (17)$$

2  The critical axial load, $P_{cr}$, is calculated as

3
$$P_{cr} = \frac{\pi^2 \phi_{er}(EI)_{eff}}{(1 + \beta_d)(kH_w)^2} \qquad (18)$$

4  where in this case $\beta_d$, the ratio of factored dead load moment to total moment is zero with all

5  applied loads being considered as live loads, the resistance factor for reinforced masonry, $\phi_{er}$, is

6  0.75, and the effective length factor, k, is 1 for pinned-pinned boundaries and 0.81 for pinned-

7  fixed based on Table B.1 of CSA S304-14 (2014).

8  The P-Δ approach can be applied using the service moment and load in (2) through (5). When

9  the P-Δ method is applied for moment magnification the following rigidity coefficient should be

10  applied to the effective stiffness used to calculate the displacements.

11
$$\frac{\phi_{er}(EI)_{eff}}{(1 + \beta_d)} \qquad (19)$$

12  ***Wall calculations***

13  Comparison of the methods for calculating the maximum displacements are shown in Table 9 for

14  the pinned-pinned (pp) condition and pinned-fixed (pf) conditions under the maximum test loads

15  for both axial loading (A) and combined axial and horizontal out-of-plane loading (A+OOP).

16  The moment magnifier and P-Δ methods have each been applied to the simplified and detailed

17  calculation approaches.  While the simplified displacement calculations are intended for

18  application only at the mid-height of the wall, they have also been applied at the locations of

19  maximum displacement for the pinned-fixed walls.  The detailed displacement calculations have

20  been applied to the gross cross-sectional properties, as well as the effective section properties

1     calculated using the methods outlined above. Calculations based on the gross cross sectional

2     stiffness are intended only for comparison to illustrate the effect of cracking on the behaviour.

3     Considering the simplified calculation approach, the addition of an out-of-plane load causes a

4     significant increase in the service moment at mid-height when the base support is pinned, leading

5     to large displacements under combined loading.  Similarly, when considering the detailed

6     calculation method, the addition of the out-of-plane load significantly reduces the effective

7     stiffness when the wall is pinned-pinned, again leading to large displacements.  The impact of

8     the out-of-plane load is reduced when the base is considered fixed in the calculations as both the

9     moment and stiffness are less affected by the additional load.  For walls with a fixed base the

10     detailed displacement calculation approach using $(EI)_{eff,1}$ consistently produces the largest

11     displacements. This is because the limit of $0.25(EI)_o$ consistently governs when calculating

12     $(EI)_{eff,1}$ causing a much lower stiffness than determined with the other methods. Whereas there

13     are no limiting values on $(EI)_{eff,2,}$ and the solid cross-sectional properties, $(EI)_o,$ are used for

14     condition where cracking has not occurred.

15     When applying the simplified calculation method at the full test load, the service moment

16     exceeded the cracking moment for both pinned-pinned load cases, while the service moment was

17     consistently less than the cracking moment when the base support was fixed.  This led to

18     different equations being applied for the two support conditions and the effect of cracking being

19     considered for the pinned base walls. This was consistent under 75% of the total test load, while

20     under 50% of the total test load the service load was less than the cracking moment for the case

21     of axial load alone for the pinned-pinned wall. Comparing the Moment Magnifier and P-$\Delta$

22     approaches under different load magnitudes shows that if the service moment exceeds the

23     cracking moment the moment magnification approach produces larger displacement, whereas

24

1    when the service moment does not produce cracking the P-Δ magnification approach produces

2    larger displacements.  For all detailed displacement calculations, the P-Δ magnification approach

3    produced larger displacements than the moment magnifier equation.

4    Comparison of the hand calculations with the corresponding test results is given in Table 10.

5    The maximum of the two displacements at $0.4H_w$ and $0.6H_w$ was used for the mid-height

6    displacement, and the maximum of the displacement at $0.6H_w$ and $0.8H_w$ was used for the

7    displacement at x of 845 mm and 948 mm from the top of the wall.  The accuracy of the

8    calculation methods when compared with the maximum observed displacement values is shown.

9    When the ratio is greater than 1 the value is highlighted.  The simplified method with P-Δ

10   magnification is shown to be in reasonable agreement with the axial test load results, but with

11   greater overestimation when an out-of-plane load is applied.

12   The simplified calculations for out-of-plane displacements were found to agree with the testing

13   results in the pinned-pinned case, having ratios primarily between 1.3 and 4.2. The CSA S304-14

14   (2014) requirement for a minimum value of $(EI)_{eff\,1}$ leads to displacement ratios between 4.46

15   and 11.4 when utilized with the P-Δ magnification method, and ratios between 2.7 and 7.0 using

16   the moment magnifier method.  The second approach for calculating the effective section

17   property $(EI)_{eff\,2}$ has no limits applied, and gives ratios between 1.5 and 4.4 using the moment

18   magnifier method, and between 2.2 and 7.2 with the P-Δ magnification method.

19   Agreement between the pinned-fixed test results and hand calculations vary greatly.  The

20   simplified method is not intended for application at positions other than 0.5H and gives

21   displacement ratios between 0.3 and 2.0.  Use of the cross-sectional property $(EI)_{eff\,1}$ again gives

22   consistently conservative results due to the minimum permissible value required in CSA S304-14

23   (2014).  Use of $(EI)_{eff\,1}$ with the moment magnifier method gives ratios between 1.3 and 3.9, and

25

1    between 2.2 and 6.8 with the P-$\Delta$ magnification method. Use of the second approach for

2    calculating the effective section property $(EI)_{eff\,2}$ consistently gives displacements below the test

3    values with ratios between 0.3 and 1.1 when the moment magnifier method is used.  The results

4    vary between 0.5 and 1.7 when $(EI)_{eff\,2}$ is used with the P-$\Delta$ magnification method.

5    However, were the pinned-pinned calculation approach to be applied to the pinned-fixed test

6    results, as would be the case for walls having slenderness ratios of 30 or greater, the calculations

7    would greatly overestimate the out-of-plane displacements as shown in Table 11. The

8    overestimation in the calculations varies with the method used. All calculated displacements

9    exceed the test displacements and the calculations are increasingly conservative when out-of-

10   plane loads are applied.

11   **DISCUSSION**

12   The behaviour of a concrete masonry wall has been shown to be greatly affected by the support

13   conditions at the base of the wall.  Although no additional measures than would occur in normal

14   practice were taken to ensure a moment connection at the wall base, testing demonstrated that a

15   displaced profile similar to that of a fixed base occurs when that support is not forced to be a pin.

16   Actual wall behaviour for walls up to 2.4 m was demonstrated to be more accurately described

17   by an intermediate condition at the base that is much closer to fixed than pinned. In normal

18   construction, there is steel reinforcement embedded into the foundation, as provided here, and

19   rotation of the foundation would be unlikely, with foundation depth required to reach below the

20   frost line. The assumption of a pinned connection at the base is clearly overly conservative for

21   walls up to 2.4 m in height with a single bond beam at the base of the wall and two vertical

22   dowels into the foundation, as the test walls deviate from the pinned-pinned condition with the

23   maximum out-of-plane displacements occurring between 0.8 and 0.6 of the total height when

26

1    axial and combined axial and out-of-plane loads are applied. A significant increase in the

2    displacements occurs when the base is forced to behave as pinned for the tested load cases.

3    Previous studies focused primarily on testing walls with pinned based conditions. As

4    demonstrated through this testing, a pinned support condition is not an accurate representation of

5    what occurs in practice. From the review of previous studies (Yokel et al. 1970; Yokel et

6    al. 1971; Cranston and Roberts 1976; Drysdale et al. 1976; Fattal and Cattaneo 1976;

7    Hatzinikolas et al. 1978; the ACI-SEASC Task Committee on Slender Walls 1982; Suwalski

8    1986; Hatzinikolas et al.1991; Mohsin and Elwi 2003; Liu and Hu 2007; and Popehn et al. 2008)

9    it has been established that the Canadian standard S304-14 (2014) underestimates the capacity of

10   concrete block masonry walls.  The use of the effective height factor of 1 and the method of

11   calculating the effective section properties has been shown to cause an overestimation of the out-

12   of-plane displacement.  The simplified CSA S304-14 (2014) calculations give an accurate

13   assessment the out-of-plane displacements when the pinned-pinned tests are compared to pinned-

14   pinned calculations.  However, the simplified calculation method yields a poor approximation of

15   the out-of-plane displacements for pinned-fixed walls, both over and underestimating the actual

16   displacements. When the simplified pinned base calculations are applied to walls without a

17   pinned support forced at the base, the displacements are over-estimated by a minimum factor of

18   2 for axial loading alone, and up to a factor of 26 when an out-of-plane load is applied.  Ignoring

19   the moment resistance of masonry walls on a rigid surface leads to overdesign and material

20   waste.

21   An important observation from this testing was the difficulty with which the displacements were

22   maintained at zero at the top of the wall.  Flexibility in the supporting frame led to adjustments

23   being required after the application of vertical and out-of-plane load.  Further study of in-situ

27

1 wall behaviour would better inform the interaction of the floor/ceiling diaphragm and

2 perpendicular walls with a wall subjected to out-of-plane loading. Testing of walls of greater

3 heights and slenderness ratios would be ideal to establish if the deflection measurements of the

4 taller walls retain the profile of a pinned-fixed wall profile under the same loading.

5 Overall, results of the work to date indicate that the provisions for slender walls in the Canadian

6 standard S304-14 (2014) need to be re-examined to ensure more efficient use of masonry.

## ACKNOWLEDGEMENTS

## REFERENCES

13 ACI-SEASC Task Committe on Slender Walls. 1982. Test Report on Slender Walls. American Concrete

14 Institute Structural Engineers Association of Southern California, Los Angles, C.A.

15 American Society for Testing and Materials Committee E06. 2015. ASTM E72-15 Standard Test

16 Methods of Conducting Strength Tests of Panels for Building Construction. ASTM International, West

17 Conshohocken, P.A.

18 Canadian Standard Association. 2014. S304.1-14 Design of Masonry Structures. Canadian Standards

19 Association, Mississauga, O.N.

20 Canadian Standard Association. 2014. A23.3-14 Design of Concrete Structures. Canadian Standards

21 Association, Mississauga, O.N.

1    Chapman, J. C. and Slatford, J. 1957. The elastic buckling of brittle columns. Proceeding of the

2    Institution of Civil Engineers, **6**(1): 107-125.

3    Cranston, W. B. and Roberts, J. J. 1976. The Structural Behaviour of Concrete Masonry Reinforced and

4    Unreinforced. Structural Engineer, **54**: 423-436.

5    Dizhur, D., Derakhshan, H., Ingham, J. M. and Griffith, M. C. 2009. In situ Out-of-Plane Testing of

6    Unreinforced Masonry Partition Walls. *In* Proceedings of 11th Canadian Masonry Symposium, Toronto

7    O.N. 31 May - 3 June 2009. pp. 10.

8    Drysdale, R.G., Hamid, A. A. 2005. Masonry Structures Behaviour and Design: Canadian Edition,

9    Canadian Masonry Design Centre, Mississauga, O.N.

10   Drysdale, R. G., Sallam, S. E. A. and Karaluk, E. 1976. Design of Masonry Walls and Columns for

11   Combined Axial Load and Bending Moment. *In* Proceedings of 1st Canadian Masonry Symposium,

12   Calgary, A.B., 7-10 June 1976. pp. 394-408.

13   Fattal, S. G. and Cattaneo, L. E. 1976. Structural Performance of Masonry Walls under Compression and

14   Flexure. Building Science Series 73, US National Bureau of Standards, Washington, D.C.

15   Hatzinikolas, M., Neis, V. V. and Ghosh, S. 1991. Strength Test on Slender Plain Block Masonry Walls

16   with Veneer Wythes, Canadian Journal of Civil Engineering, **18**(5), 739-748.

17   Hatzinikolas, M. A., Longworth, J. and Warwaruk, J. 1978. Concrete Masonry Walls. Structural

18   Engineering Report 70, University of Alberta, Edmonton, A.B.

19   Hendry, A. W. 1990. Structural Masonry. Macmillan Education, Ltd. London.

20   Liu, Y. and Hu, K. 2007. Experimental Study of Reinforced Masonry Walls Subjected to Combined Axial

21   and Out-of-Plane Bending. Canadian Journal of Civil Engineering, **34**: 1486-1494.

1    McDowell, E. L., McKee, K. E. and Seven, E. 1956. Arching action theory of masonry walls. ASCE

2    Journal of the Structural Divison, **82**(ST2): 915.911-915.918.

3    Mohsin, E. and Elwi, A. E. 2003. Effect of implied fixity at masonry block wall support interface on

4    stability of load bearing walls. *In* Proceedings of 9th North American Masonry Conference, Clemson,

5    S.C., 1-4 June 2003, pp. 884-895.

6    Ojinaga, J., and Turkstra, C. J. 1982. Design of reinforced masonry walls and columns for gravity loads.

7    Canadian Journal of Civil Engineering, **9**: 84-95.

8    Popehn, J. R. B., Schultz, A. E., Lu, M. and Storlarski, H. K. 2008. Influence of Transverse Loading on

9    the Stability of Slender Ureinforced Masonry Walls. Engineering Structures, **30**(10): 2830-2839.

10   Sahlin, S. 1971. Stability of concentrically loaded masonry walls. Structural Masonry. Prentice-Hall, Inc.,

11   Englewood Cliffs, N.J.

12   Suwalski, P. D. 1986. Capacity of eccentrically loaded slender concrete block walls. M.Sc. thesis,

13   Department of Civil Engineering, McMaster University, Hamilton O.N.

14   Walsh, K. Q., Dizhur, D. Y., Giongo, I., Derakhshan, H. and Ingham, J. M. 2017.  Effect of boundary

15   conditions and other factors on URM wall out-of-plane behaviour. SESOC Journal, **30**(1): 57-81.

16   Yokel, F. Y. 1971. Stability and load capacity of members with no tensile strength. ASCE Journal of the

17   Structural Division, **97**(ST7): 1913-1926.

18   Yokel, F. Y., Mathey, R. G. and Dikkers, R. D. 1970. Compressive Strength of Slender Concrete

19   Masonry Walls, Building Science Series 33, US National Bureau of Standards, Washington, D.C.

20   Yokel, F. Y., Mathey, R. G. and Dikkers, R. D. 1971. Strength of Masonry Walls Under Compressive and

21   Transverse Loads, Building Science Series 34, US National Bureau of Standards, Washington, D.C.

22

1 **Table 1: Overview of experimental programs with concentric and eccentric axial loading**

| Author | Year | t [mm] | h [m] | h/t [-] | $A_s$ | $e_1/t$ [-] | $e_1/e_2$ [-] | Support |
|--------|------|--------|-------|---------|-------|-------------|---------------|---------|
| Yokel, Mathey, Dikkers | 1970 | 194 | 3.1 | 15.7 | - | 0, 0.17, 0.25, 0.33 | 1 | pinned-fixed |
| | | | 4.9 | 25.2 | | 0, 0.17, 0.25, 0.33 | 1 | |
| | | | 6.1 | 31.5 | | 0, 0.17, 0.25, 0.33 | 1 | |
| | | 143 | 3.1 | 21.3 | 2#15 | 0, 0.17, 0.25, 0.33 | 1 | |
| | | | 4.9 | 34.1 | | 0, 0.17, 0.25, 0.33 | 1 | |
| | | | 6.1 | 42.7 | | 0, 0.17, 0.25, 0.33 | 1 | |
| Cranston, Roberts | 1976 | 140 | 2.6 | 18.7 | - | 0, 0.14, 0.29, 0.36 | 1 | pinned-pinned fixed-fixed |
| | | | | | | 0 | 1 | |
| Drysdale | 1976 | 143 | 2.9 | 20.0 | - | 0, 0.17, 0.33, 0.35 | 1 | pinned-pinned |
| | | | | | 1#15 | 0.17, 0.33, 0.5 | 1 | |
| Fattal, Cattaneo | 1976 | 143 | 2.5 | 17.1 | - | 0, 0.08, 0.17, 0.25, 0.33 | 1 | pinned-pinned |
| | | | | | | 0.33 | 0 | |
| | | | | | | 0.33 | -1 | |
| Hatzinikolas, Longsworth, Warwaruk | 1978 | 194 | 2.7 | 13.8 | - | 0, 0.17, 0.33, 0.39 | 1 | pinned-pinned |
| | | | 4.7 | 24.2 | | 0, 0.17 | 1 | |
| | | | 3.5 | 18.0 | | 0.17, 0.33, 0.39 | 0 | |
| | | | 2.7 | 13.8 | | 0.17, 0.33 | -1 | |
| | | | 3.5 | 18.0 | | 0.17, 0.33, 0.38 | -1 | |
| | | | 2.7 | 13.8 | 3#9 (imp.) | 0.17, 0.33, 0.39, 0.46 | 1 | |
| | | | 3.1 | 15.9 | | 0, 0.17, 0.33, 0.39, 0.46 | 1 | |
| | | | 3.5 | 18.0 | | 0, 0.17, 0.33, 0.39, 0.46 | 1 | |
| | | | 4.7 | 24.0 | | 0, 0.17, 0.33, 0.39, 0.46 | 1 | |
| | | | 3.5 | 18.0 | 3#6 (imp.) | 0, 0.17, 0.33, 0.39, 0.46 | 1 | |
| | | | 3.5 | 18.0 | 3#3 (imp.) | 0, 0.17, 0.33, 0.39, 0.46 | 1 | |
| | | | 3.5 | 18.0 | | 0.17, 0.33, 0.39, 0.46 | -1 | |
| Suwalski | 1986 | 190 | 3.2 | 16.8 | - | 0.07, 0.17, 0.33, 0.35 | 1 | pinned-pinned |
| | | | | | 2#15 | 0.18, 0.32, 0.34, 0.5, 0.54, 0.75 | 1 | |
| Hatzinikolas | 1991 | 140 | 4.2 | 30.0 | - | 0, 0.18, 0.36 | 1 | pinned-pinned |
| Mohsin, Elwi | 2003 | 190 | 5.43 | 28.6 | 2#15 | 0.33 | 0 | pinned/ part. fixed - pinned |
| | | | 6.44 | 33.9 | | | 0 | |
| Liu, Hu | 2007 | 140 | 2.4 | 17.1 | 2#10 | 0, 0.17, 0.25, 0.33 | 1 | pinned-pinned |
| | | | | | | 0.17, 0.25, 0.33 | 0 | |
| | | | | | | 0.17, 0.25, 0.33 | -1 | |

2

1 **Table 2: Overview of experimental programs with combined axial and out-of-plane loading**

| Author | Year | t [mm] | h [m] | h/t [-] | $A_s$ | e/t [-] | Axial Load [kN/m] | Support |
|---|---|---|---|---|---|---|---|---|
| Yokel, Mathey, Dikkers | 1971 | 194 [1] 194 [2] 194 [3] | 2.5 | 12.9 | - | 0 0 0 | 0, 74, 148, 223, 445, 501, 548 0, 148, 278, 482, 556 0, 93, 185, 371, 556, 1853, 1965, 2213 | pinned-partially fixed |
| Fattal, Cattaneo | 1976 | 143 | 2.5 | 17.1 | - | 0 0.25 | 0, 111, 223 111 | pinned-pinned |
| ACI-SEASC Task Committee on Slender Walls | 1982 | 244 194 143 | 7.3 7.4 7.3 | 30.0 38.0 51.2 | 5#4 (imp.) | 0.81 0.89 1.03 | 4.67, 12.55 4.67, 12.55 4.67 | pinned-pinned |
| Popehn et al. | 2008 | 92.7 | 3.5 | 37.5 | - | 0 | 83.0, 165.6, 276.5, 415.9 | pinned-pinned |

[1] hollow blocks, Type N mortar

[2] hollow blocks, high bond mortar

[3] solid blocks, Type N mortar

2

1    **Table 3: Details and results of the unreinforced walls tested by Hatzinikolas (1978)**

| t [mm] | f'$_m$ [MPa] | b [m] | h [m] | h/t [-] | A$_s$ | e$_1$/t [-] | e$_1$/e$_2$ [-] | exp. Failure Load [kN/m] | E$_{exp}$ [N/mm²] | I$_0$ [mm⁴/m] | Euler Load [kN/m] | P$_{cr}$ [kN/m] | P$_r$ [kN/m] | ratio [-] |
|---|---|---|---|---|---|---|---|---|---|---|---|---|---|---|
| 194 | 13.0 | 1.0 | 2.7 | 13.8 | - | 0 | 1 | 1114 | 7722 | 4.2E+08 | 4425 | 1098 | 322 | 3.46 |
| | | | | | - | 0.17 | 1 | 708 | | | | | 280 | 2.53 |
| | | | | | - | 0.33 | 1 | 357 | | | | | 157 | 2.27 |
| | | | | | - | 0.39 | 1 | 116 | | | | | 81 | 1.43 |
| | | | 3.5 | 18.0 | - | 0.17 | 0 | 764 | 7722 | 4.2E+08 | 2633 | 653 | 299 | 2.56 |
| | | | | | - | 0.33 | 0 | 555 | | | | | 237 | 2.34 |
| | | | | | - | 0.39 | 0 | 68 | | | | | 151 | 0.45 |
| | | | 4.7 | 24.2 | - | 0 | 1 | 924 | 7722 | 4.2E+08 | 1460 | 362 | 245 | 3.77 |
| | | | | | - | 0.17 | 1 | 534 | | | | | 203 | 2.63 |
| | | | 2.7 | 13.8 | - | 0.17 | -1 | 980 | 7722 | 4.2E+08 | 4425 | 1098 | 308 | 3.18 |
| | | | | | - | 0.33 | -1 | 696 | | | | | 237 | 2.94 |
| | | | 3.5 | 18.0 | - | 0.17 | -1 | 811 | 7722 | 4.2E+08 | 2633 | 653 | 308 | 2.63 |
| | | | | | - | 0.33 | -1 | 671 | | | | | 237 | 2.83 |
| | | | | | - | 0.39 | -1 | 574 | | | | | 151 | 3.80 |
| | | | | | - | 0.39 | -0.9 | 670 | | | | | - | - |

▓  buckling

2

1    **Table 4: Details and results of the walls tested by the ACI-SEASC Committee (1982)**

| t [mm] | f'$_m$ [MPa] | b [m] | h [m] | h/t [-] | A$_s$ | e/t [-] | P [kN/m] | Ult. Horiz. Load [kN/m²] | Deflection [mm] | M$_{(P\Delta+Hl^2/8)}$ [kNm/m] | M$_r$ [kNm/m] | ratio [-] | M$_{f,tot}$ [kNm/m] |
|---|---|---|---|---|---|---|---|---|---|---|---|---|---|
| 244 | 17 | | 7.3 | 30.0 | | 0.81 | 4.67 | 4.8 | 434 | 34.9 | 20.8 | 1.7 | 34.7 |
| | | | | | | 0.81 | 12.55 | 4.2 | 203 | 33.0 | 21.6 | 1.5 | 35.3 |
| | | | | | | 0.81 | 12.55 | 4.8 | 483 | 40.5 | 21.6 | 1.9 | 39.9 |
| 194 | 17.9 | 1.2 | 7.4 | 38.0 | 5#4 (imp) | 0.89 | 12.55 | 4.4 | 284 | 35.8 | 16.8 | 2.1 | 42.0 |
| | | | | | | 0.89 | 12.55 | 3.9 | 262 | 32.2 | 16.8 | 1.9 | 37.5 |
| | | | | | | 0.89 | 4.67 | 5.4 | 376 | 39.5 | 16.3 | 2.4 | 41.3 |
| 143 | 22 | | 7.3 | 51.2 | | 1.03 | 4.67 | 3.0 | 450 | 22.8 | 11.8 | 1.9 | 24.5 |
| | | | | | | 1.03 | 4.67 | 1.9 | 404 | 15.2 | 11.8 | 1.3 | 15.8 |
| | | | | | | 1.03 | 4.67 | 2.3 | 279 | 17.3 | 11.8 | 1.5 | 19.0 |

2

34

1 **Table 5: Mortar Mixed According to Volume Proportion Specifications of CSA-A179-2014**

| Mortar type | Portland cement | Hydrated lime or lime putty | Aggregate measured in damp, loose state |
|---|---|---|---|
| S | 1 | ½ | 3-½ |

2

1 **Table 6: Grout Mixed According to Volume Proportion Specification of CSA-A179-2014**

| Grout type | Portland cement | Hydrated lime or lime putty | Aggregate measured in damp, loose state | |
|---|---|---|---|---|
| | | | Fine aggregate (sand) | Coarse aggregate |
| Coarse | 1 | 0 to 1/10 | 2-1/4 to 3 times the sum of the cementitious material | 1 to 2 times the sum of the cementitious material |

2

36

1

**Table 7: Material Test Results**

| Material | Avg. Comp. Strength [MPa] | C.O.V. [%] | Effective Comp. Strength [MPa] |
|---|---|---|---|
| Block | 22.15 | 7.7 | 18.52 |
| Mortar | 12.35 | 6.6 | 10.32 |
| Grout | 22.22 | 3.4 | 18.58 |
| Prism | 18.21 | 4.9 | 15.22 |

2

37

1

**Table 8: Maximum Displacement [mm]**

| Base Support | Displacement [mm] | | | | | | | |
|---|---|---|---|---|---|---|---|---|
| | Axial | | | | Axial + Out-of-Plane | | | |
| | Test | | | | Test | | | |
| | 100% | | 75% | 50% | 100% | | 75% | 50% |
| | Min | Max | | | Min | Max | | |
| Fixed | 0.34 | 0.88 | 1.13 | 0.28 | 0.79 | 1.17 | 1.08 | 0.45 |
| Pinned | 1.90 | 3.81 | 1.36 | 0.79 | 6.59 | 9.82 | 4.38 | 2.52 |
| Pinned/Fixed Ratio | 5.57 | 4.31 | 1.20 | 2.84 | 8.34 | 8.40 | 4.06 | 5.66 |

2

38

1 **Table 9: Displacement Calculation Summary**

| Test Load Mag. | Case | x [mm] | M-Mag Displacement [mm] | | | | | P-Δ Displacement [mm] | | | | |
|---|---|---|---|---|---|---|---|---|---|---|---|---|
| | | | Simplified | | Detailed | | | Simplified | | Detailed | | |
| | | | $(EI)_o$ | $(EI)_{cr}$ | $(EI)_o$ | $(EI)_{eff\,1}$ | $(EI)_{eff\,2}$ | $(EI)_o$ | $(EI)_{cr}$ | $(EI)_o$ | $(EI)_{eff\,1}$ | $(EI)_{eff\,2}$ |
| 100% | pp A | 1336 | 8.92 | | 2.65 | 12.34 | 10.70 | 6.94 | | 3.64 | 20.59 | 17.24 |
| | pp A+OOP | 1336 | 29.88 | | 3.96 | 26.55 | 31.70 | 29.12 | | 4.73 | 43.78 | 57.27 |
| | pf A | 845 | 0.82 | | 0.59 | 2.34 | 0.59 | 1.14 | | 0.94 | 3.91 | 0.94 |
| | pf A+OOP | 948 | 1.11 | | 0.86 | 3.46 | 0.86 | 1.54 | | 1.32 | 5.47 | 1.32 |
| | pf A | 1268 | 0.41 | | 0.49 | 1.98 | 0.49 | 0.57 | | 0.79 | 3.27 | 0.79 |
| | pf A+OOP | 1268 | 0.93 | | 0.78 | 3.14 | 0.78 | 1.29 | | 1.18 | 4.89 | 1.18 |
| 75% | pp A | 1336 | 4.34 | | 1.89 | 8.79 | 5.21 | 2.80 | | 2.70 | 14.46 | 7.95 |
| | pp A+OOP | 1336 | 18.23 | | 2.74 | 18.37 | 19.34 | 17.08 | | 3.50 | 29.53 | 31.60 |
| | pf A | 845 | 0.62 | | 0.44 | 1.76 | 0.44 | 0.85 | | 0.70 | 2.89 | 0.70 |
| | pf A+OOP | 948 | 0.84 | | 0.65 | 2.59 | 0.65 | 1.14 | | 0.98 | 4.05 | 0.98 |
| | pf A | 1268 | 0.31 | | 0.37 | 1.48 | 0.37 | 0.42 | | 0.59 | 2.43 | 0.59 |
| | pf A+OOP | 1268 | 0.70 | | 0.59 | 2.35 | 0.59 | 0.96 | | 0.89 | 3.63 | 0.89 |
| 50% | pp A | 1336 | 1.00 | | 1.20 | 5.58 | 1.20 | 1.24 | | 1.78 | 9.06 | 1.78 |
| | pp A+OOP | 1336 | 8.85 | | 1.70 | 11.37 | 9.39 | 8.03 | | 2.31 | 17.89 | 14.31 |
| | pf A | 845 | 0.41 | | 0.29 | 1.17 | 0.29 | 0.56 | | 0.47 | 1.90 | 0.47 |
| | pf A+OOP | 948 | 0.56 | | 0.43 | 1.73 | 0.43 | 0.76 | | 0.65 | 2.67 | 0.65 |
| | pf A | 1268 | 0.21 | | 0.25 | 0.99 | 0.25 | 0.28 | | 0.39 | 1.60 | 0.39 |
| | pf A+OOP | 1268 | 0.47 | | 0.39 | 1.57 | 0.39 | 0.63 | | 0.59 | 2.39 | 0.59 |

2

**Table 10: Ratio of Calculated to Test Displacement**

| Test Load Mag. | Case | x [mm] | M-Mag Displacement Ratio | | | | P-Δ Displacement Ratio | | | |
|---|---|---|---|---|---|---|---|---|---|---|
| | | | Simplified | Detailed | | | Simplified | Detailed | | |
| | | | $(EI)_o (EI)_{cr}$ | $(EI)_o$ | $(EI)_{eff\,1}$ | $(EI)_{eff\,2}$ | $(EI)_o (EI)_{cr}$ | $(EI)_o$ | $(EI)_{eff\,1}$ | $(EI)_{eff\,2}$ |
| 100% | pp A | 1336 | 2.34 | 0.70 | 3.24 | 2.81 | 1.80 | 0.96 | 5.40 | 4.52 |
| | pp A+OOP | 1336 | 3.04 | 0.40 | 2.70 | 3.23 | 2.96 | 0.48 | 4.46 | 5.83 |
| | pf A | 845 | 0.93 | 0.66 | 2.65 | 0.66 | 1.29 | 1.06 | 4.42 | 1.06 |
| | pf A+OOP | 948 | 0.95 | 0.74 | 2.96 | 0.74 | 1.32 | 1.13 | 4.68 | 1.13 |
| | pf A | 1268 | 0.82 | 0.56 | 3.94 | 0.98 | 1.13 | 1.58 | 6.52 | 1.58 |
| | pf A+OOP | 1268 | 0.97 | 0.67 | 3.27 | 0.82 | 1.34 | 1.23 | 5.10 | 1.23 |
| 75% | pp A | 1336 | 3.19 | 1.39 | 6.47 | 3.83 | 2.06 | 1.99 | 10.63 | 5.85 |
| | pp A+OOP | 1336 | 4.16 | 0.63 | 4.19 | 4.41 | 3.90 | 0.80 | 6.74 | 7.21 |
| | pf A | 845 | 0.55 | 0.39 | 1.56 | 0.39 | 0.75 | 0.62 | 2.56 | 0.62 |
| | pf A+OOP | 948 | 0.77 | 0.60 | 2.40 | 0.60 | 1.06 | 0.91 | 3.75 | 0.91 |
| | pf A | 1268 | 0.27 | 0.33 | 1.31 | 0.33 | 0.37 | 0.52 | 2.15 | 0.52 |
| | pf A+OOP | 1268 | 0.65 | 0.55 | 2.18 | 0.55 | 0.89 | 0.82 | 3.36 | 0.82 |
| 50% | pp A | 1336 | 1.26 | 1.51 | 7.03 | 1.51 | 1.56 | 2.24 | 11.40 | 2.24 |
| | pp A+OOP | 1336 | 3.51 | 0.67 | 4.51 | 3.72 | 3.18 | 0.91 | 7.09 | 5.67 |
| | pf A | 845 | 1.47 | 1.05 | 4.18 | 1.05 | 1.99 | 1.67 | 6.80 | 1.67 |
| | pf A+OOP | 948 | 1.25 | 0.97 | 3.88 | 0.97 | 1.70 | 1.47 | 5.98 | 1.47 |
| | pf A | 1268 | 0.86 | 1.03 | 4.12 | 1.03 | 1.16 | 1.64 | 6.67 | 1.64 |
| | pf A+OOP | 1268 | 1.04 | 0.88 | 3.52 | 0.88 | 1.42 | 1.32 | 5.37 | 1.32 |

1
2

**Table 11: Ratio of Pinned-Pinned Calculated Displacement to Pinned-Fixed Test Displacement for all Load Cases**

| Test Load Mag. | Case | M-Mag Displacement [mm] | | | | P-Δ Displacement [mm] | | | |
|---|---|---|---|---|---|---|---|---|---|
| | | Simplified | Detailed | | | Simplified | Detailed | | |
| | | $(EI)_o \ (EI)_{cr}$ | $(EI)_o$ | $(EI)_{eff \ 1}$ | $(EI)_{eff \ 2}$ | $(EI)_o \ (EI)_{cr}$ | $(EI)_o$ | $(EI)_{eff \ 1}$ | $(EI)_{eff \ 2}$ |
| 100% | pf A | 10.09 | 3.00 | 13.96 | 12.11 | 7.85 | 4.12 | 23.29 | 19.50 |
| | pf A+OOP | 25.56 | 3.39 | 22.71 | 27.12 | 24.91 | 4.05 | 37.46 | 49.00 |
| 75% | pf A | 3.22 | 1.49 | 6.92 | 3.86 | 2.15 | 2.15 | 11.33 | 5.88 |
| | pf A+OOP | 13.93 | 2.20 | 14.42 | 14.85 | 13.12 | 2.88 | 23.03 | 23.89 |
| 50% | pf A | 3.19 | 3.83 | 17.81 | 3.83 | 3.99 | 4.70 | 21.88 | 4.70 |
| | pf A+OOP | 16.39 | 3.33 | 21.84 | 17.47 | 15.02 | 3.95 | 25.90 | 20.72 |

3

1 **LIST OF FIGURES**

(a)

(b)

Figure 1: Ratio of Experimental to Calculated Resistance for Reinforced Walls of Varying Height with Pinned-Pinned (a) and Pinned-Fixed (b) Supports
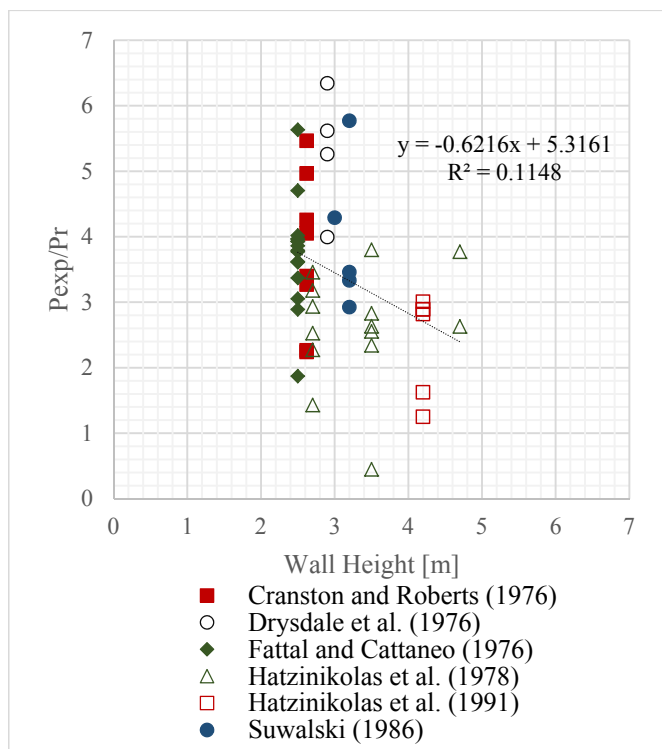
(a)
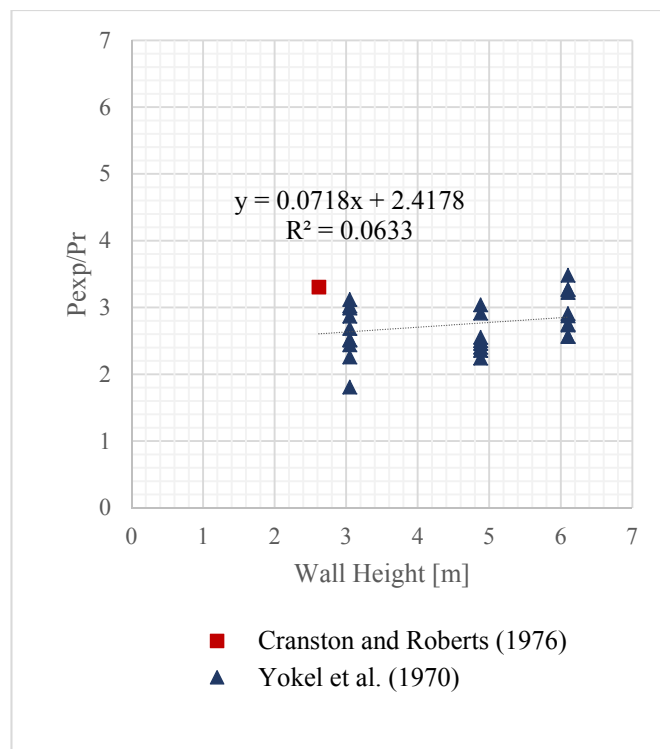
(b)

Figure 2: Ratio of Experimental to Calculated Resistance for Unreinforced Walls of Varying Height with Pinned-Pinned (a) and Pinned-Fixed (b) Supports
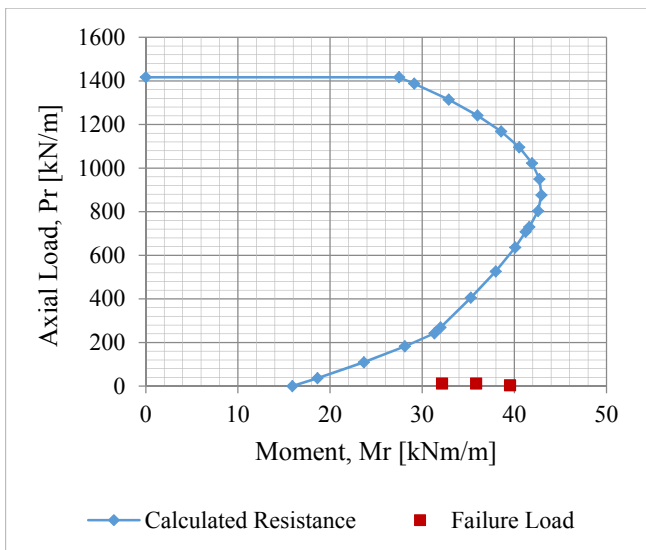
(a)
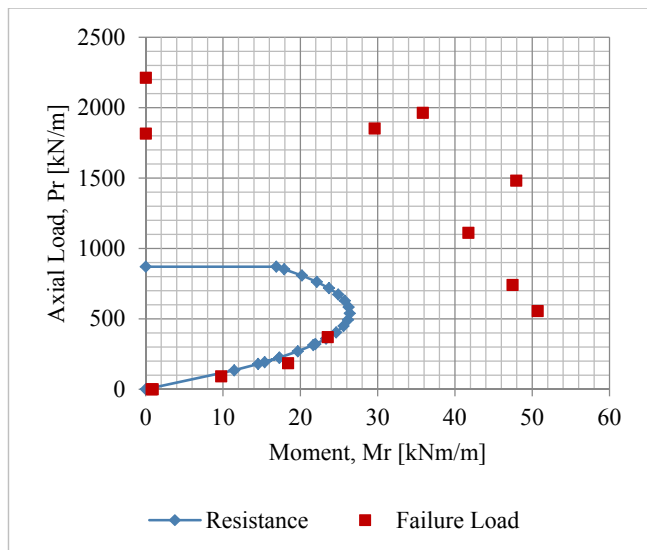


(b)

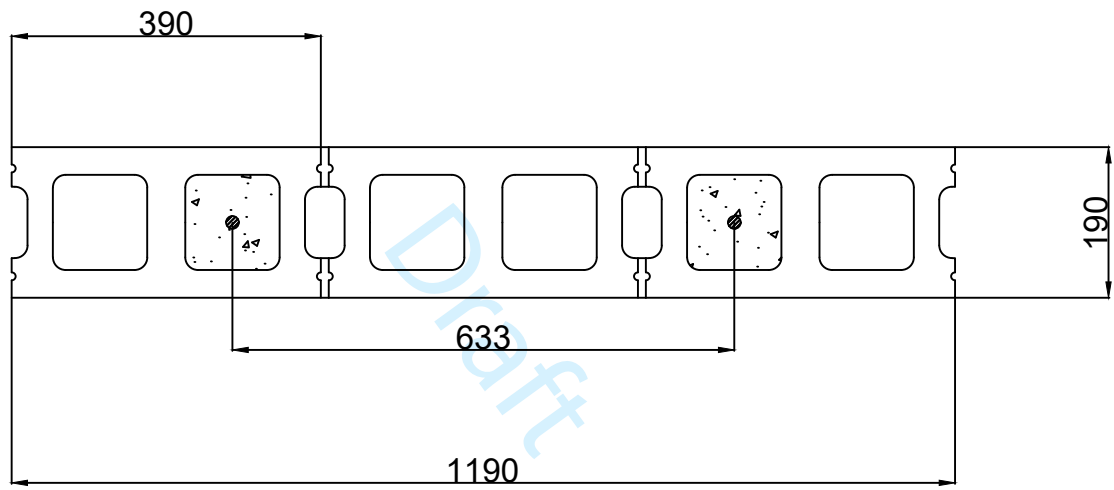Figure 3: Load-moment-interaction curves of the ACI-SEASC Committee (1982) (a) and Yokel (1971) (b)

Figure 6: Vertical Section of Wall with Pinned-Fixed Supports (a) and Base Detail Showing the Wall Placed Eccentrically in the C-channel and the Steel Beneath (b)
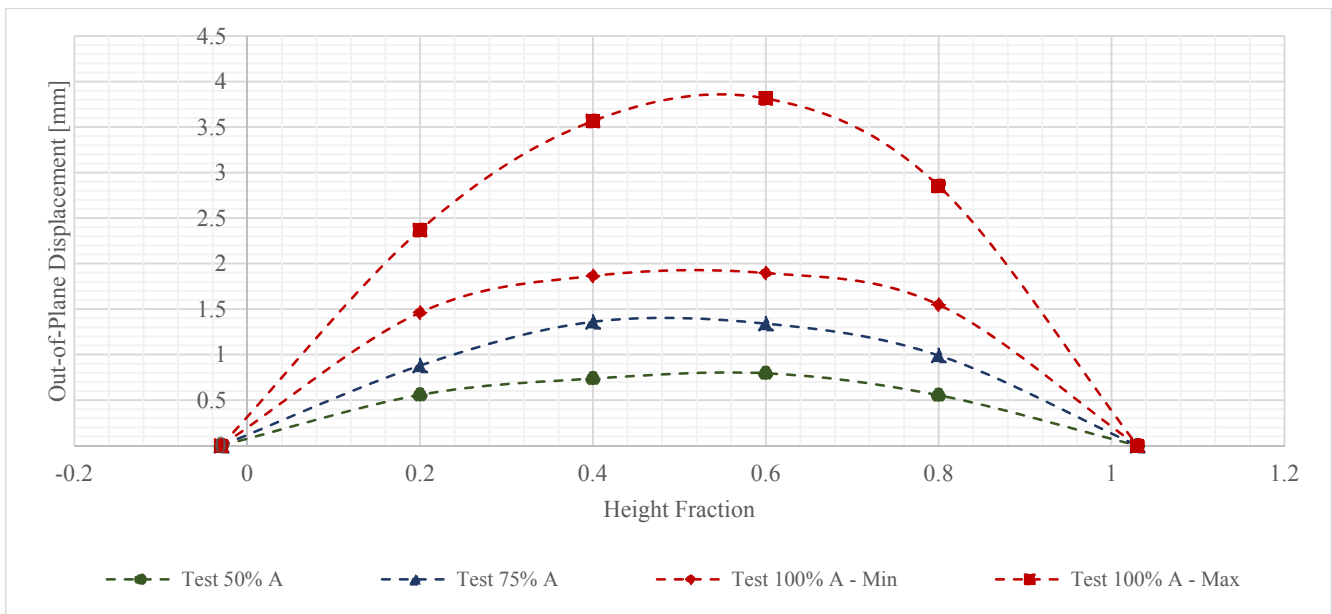
849x1128mm (72 x 72 DPI)

Figure 6: Vertical Section of Wall with Pinned-Fixed Supports (a) and Base Detail Showing the Wall Placed Eccentrically in the C-channel and the Steel Beneath (b)

786x649mm (72 x 72 DPI)
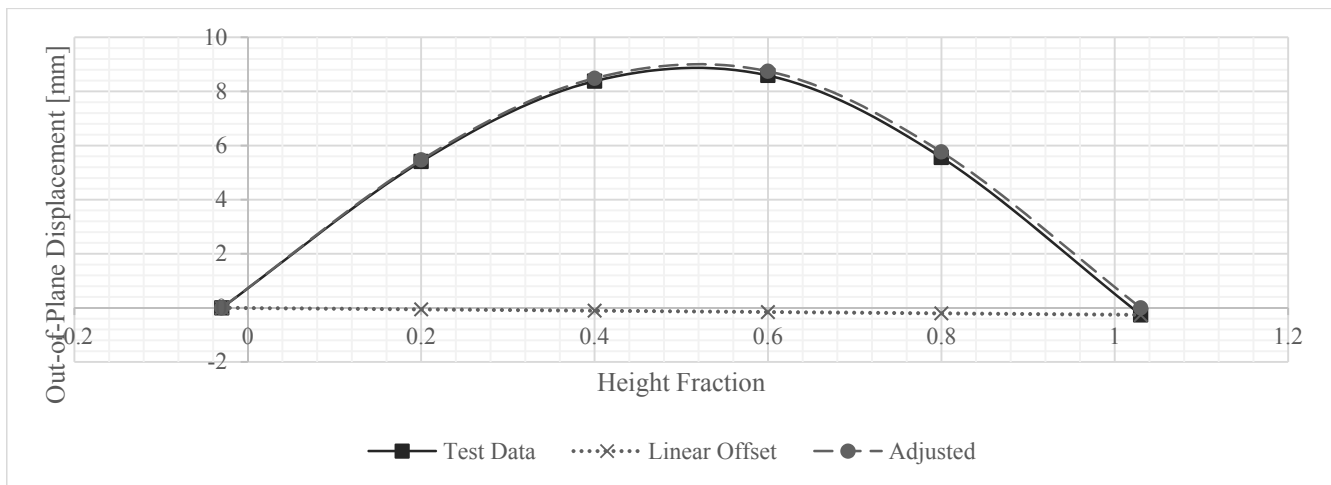
Figure 7: Linear Data Correction

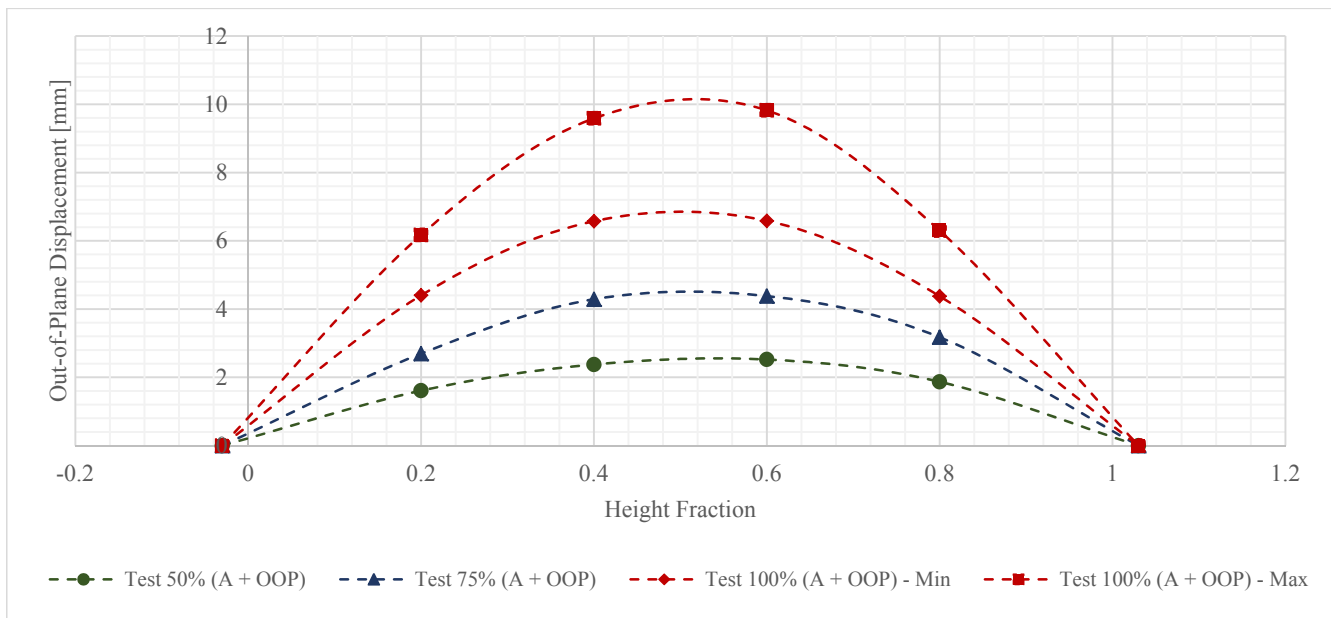Figure 8: Pinned-Pinned Displaced Profiles for Axial Load

Figure 9: Pinned-Pinned Displaced Profiles for Axial and Out-of-Plane Loads

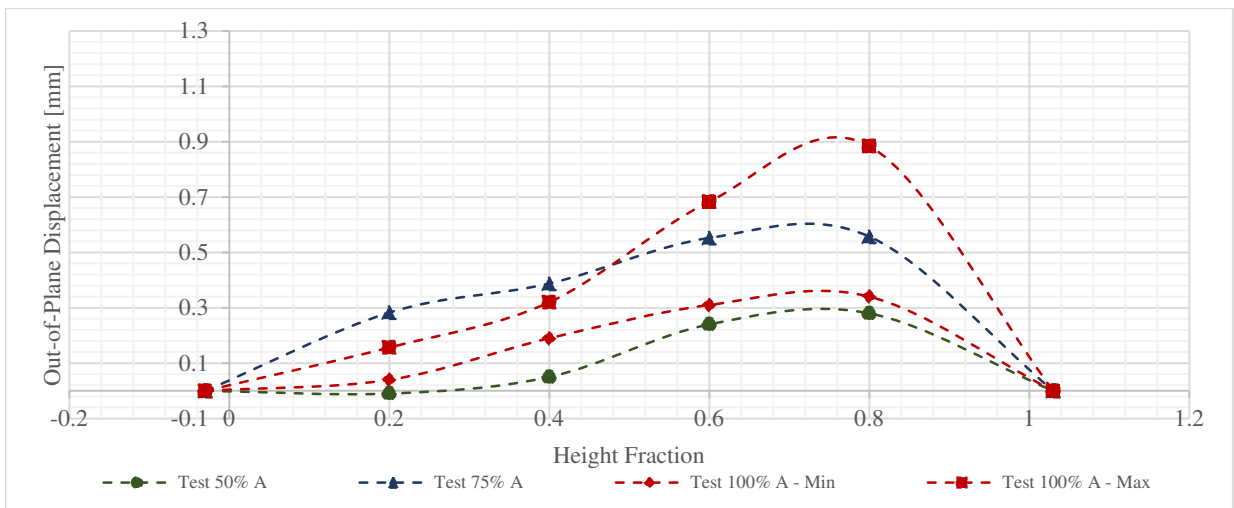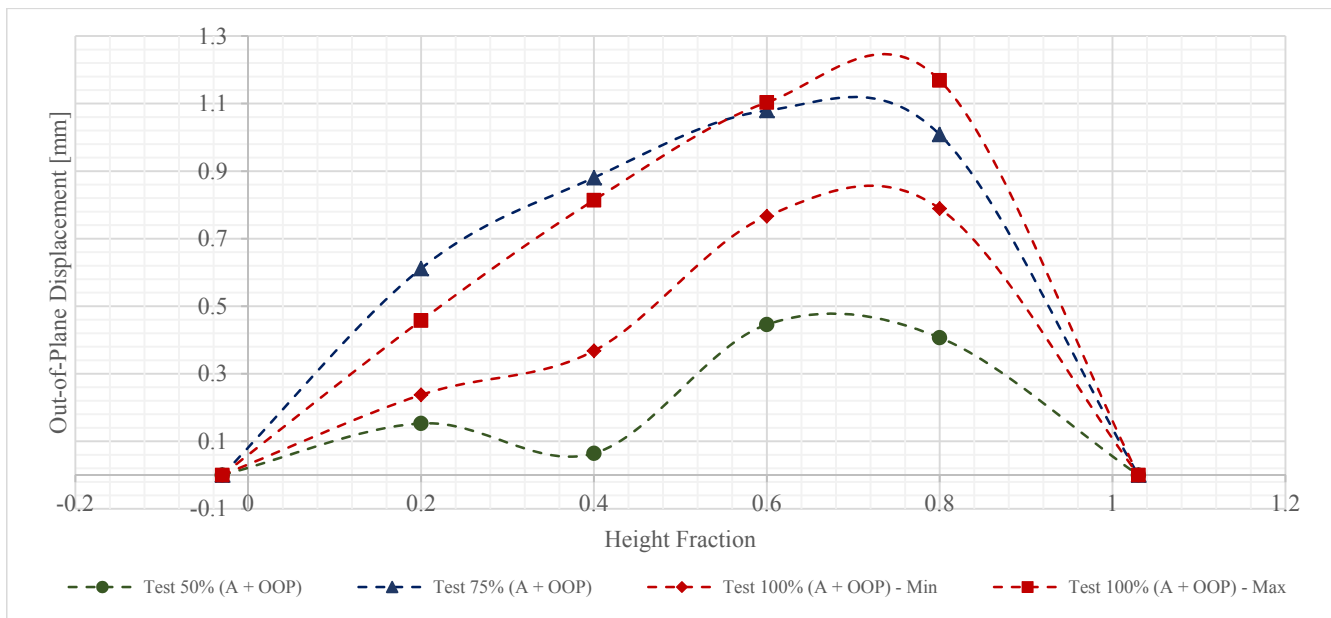Figure 10: Pinned-Fixed Displaced Profiles for Axial Load

Figure 11: Pinned-Fixed Displaced Profile for Axial and Out-of-Plane Loads